

# Performance Enhancements on a Pulsed Detonation Engine

J.M. Meyers\*, F.K. Lu<sup>†</sup>, D.R. Wilson<sup>‡</sup>

*University of Texas at Arlington, Arlington, Texas 76019*

A major problem applying detonations into aero-propulsive devices is the transition of deflagration and weak detonation into CJ detonation. The longer this transition, the longer the physical length of the engine must be to facilitate the propagation of the flame. However, lengthening of the detonation chamber can significantly increase weight, rendering the reduction of DDT (deflagration to detonation) and weak detonation transition length of great importance. One of the most common means of shortening these lengths is with the aid of a Shchelkin spiral. A simple helical apparatus, it was used in early single-shot detonation investigations to over-exaggerate wall roughness effects<sup>1</sup>. It was through empirical investigations that the reduced DDT phenomenon was observed. The present investigation explored the possibility of applying such an apparatus into an intermittent pulsed detonation device using gaseous  $C_3H_8/O_2$ . Results show significant improvements in comparison to cases without the spiral. Tests through a range of cycle frequencies up to 20Hz in oxygen-propane mixtures at 1atm demonstrated the feasibility of the Shchelkin spiral in a pulsed mode.

## Nomenclature

$A/A^*$	Critical flow nozzle area ratio
CJ	Chapman-Jouguet
$K$	Flow Coefficient
$\dot{m}$	Mass flow rate
T	Static temperature
P	Static pressure

## Introduction

There is much recent interest in the development of propulsion systems using high-frequency pulsed detonations<sup>2</sup>. An important technical challenge remains the ability to achieve consistent, repetitive detonations in a short distance. The direct initiation of detonation requires an inordinate amount of energy while a deflagration-to-detonation transition (DDT) occurs at lower energies.

For propulsion applications, the large energy requirement poses practical problems such as an energy source may not be readily available in a compact and lightweight package. Consideration therefore turns to an acceptable DDT length since it has been found that as long as transition occurs within the length of the detonation tube, the specific impulse obtained is the same as that from direct initiation<sup>3</sup>. The trade-off between energy and DDT length (or time) is crucial. A weak source would result in a long transition that causes problems

associated with length, such as reduction in cycle frequency, mixing, and engine weight. Most single-shot experiments do have transition lengths that are too excessive (0.7 to 2 m) to be practical.

One way of reducing the DDT length is to place obstacles in the detonation chamber such as orifices, channels, or spirals. It appears that some sort of DDT enhancement device may be needed for a practical PDE to be feasible. However, only a few reports exist on using these devices in a pulsed operation mode<sup>4</sup>. Most research has been done on single shot facilities. This investigation explored the behavior of a Shchelkin spiral in a pulsed detonation engine. It is expected that the rapid cycle requirements absent in single shot experiments will be affected by this obstacle.

## Experiment Setup

The experiments in this report were carried out on the University of Texas at Arlington's high frequency PDR/E facility. In operation since 1994, it utilizes a mechanical rotary valve injection system for three gas species (fuel, oxidizer, and purge). The propellants are directly detonated with the use of a high current, electric arc discharge. Near stoichiometric ratios were calibrated with the aid of two critical flow nozzles; one for fuel and one for oxidizer.

## Detonation Chamber

The detonation engine is constructed of steel tubing with an inside diameter of 7.62 cm (3 in) and outside diameter of 15.2 cm (6 in). Various lengths of 7.62, 15.2, and 30.5 cm (3, 6, and 12 in) were available. Flanges were then welded to the ends of each tube for assembly with rubber o-ring seals. Each segment was also prepared

\*Research Assistant, Aerodynamics Research Center, Box 19018, Arlington, TX 76019. Student Member AIAA.

<sup>‡</sup>Professor, Aerodynamics Research Center Director, Associate Fellow AIAA

<sup>†</sup>Department of Mechanical and Aerospace Engineering Chair, Associate Fellow AIAA.

Copyright © 2003 by J.M. Meyers, F.K. Lu, D.R. Wilson. Published by the American Institute of Aeronautics and Astronautics, Inc. with permission.

for proper instrumentation, such as pressure transducers, thermocouples, heat flux gauges, or photo-detectors. The 30.48 cm (12 in) sections allow for four equally spaced instrumentation ports along the tube. Sections of 15.24 cm (6 in) allow two ports, and 7.62 cm (3 in) sections allow one port. Another 7.62 cm (3 in) section was used to support the mounting of the arc-plug igniter. Figure 1 is a schematic of the detonation chamber for clean configuration experiments. Sections were assembled to the injection end-plate to yield a total chamber length of 53.34 cm (21 in). The first 7.62 cm (3 in) section was used to mount the igniter 3.81 cm (1.5 in) downstream of the injection wall. The following 30.48 cm (12 in) and then 15.24 cm (6 in) sections housed four ports and two ports, respectively, used for transducer mounting. The first instrumentation port is located 7.62 cm (3 in) downstream of the igniter with each of the five successive transducer ports at 7.62 cm (3 in) intervals.

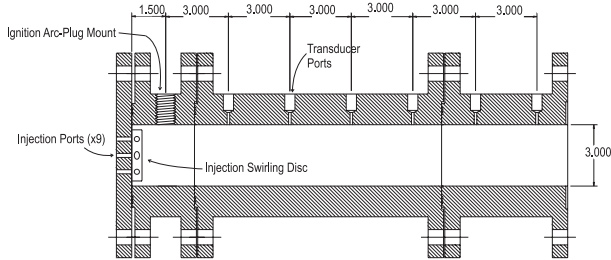


Figure 1. Clean detonation chamber configuration (dimensions in inches)

The Shchelkin spiral experimental setup is shown in Figure 2. The same detonation chamber sections were incorporated with a short spiral with a length of 20.32cm (8 in) mounted across from the ignition source. The spiral had a pitch of 15 degrees and wire diameter of 9.53 mm (3/8 in). Blockage ratio, the area of the obstruction to the area of the clean cross-section, for the spiral was about 0.21, relatively small when compared to other DDT experimental Studies<sup>5</sup>.

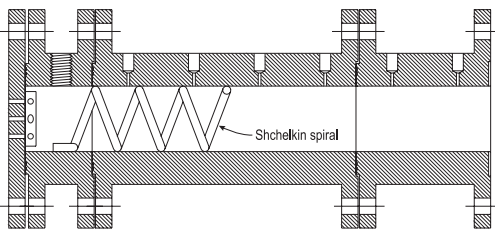


Figure 2. Detonation chamber with Shchelkin spiral installed

### Ignition System

A proper ignition system is one of the most crucial components for successful multi-cycle detonation experimentation. An ignition system for pulsed detonation engines was developed under a NASA grant as a supplement to UTA's Hypersonic Research Center in 1995. While various detonation initiation methods were considered; shock-induced detonation, explosives, lasers, electrical spark/arc, etc., it was the concept of a high current, electrical discharge that became the practical choice. The UTA ignition system consists of a series of two capacitor banks and a specialized arc-plug consisting of three electrodes similar to a common triggered spark gap device. A schematic of the ignition system is shown in figure 3.

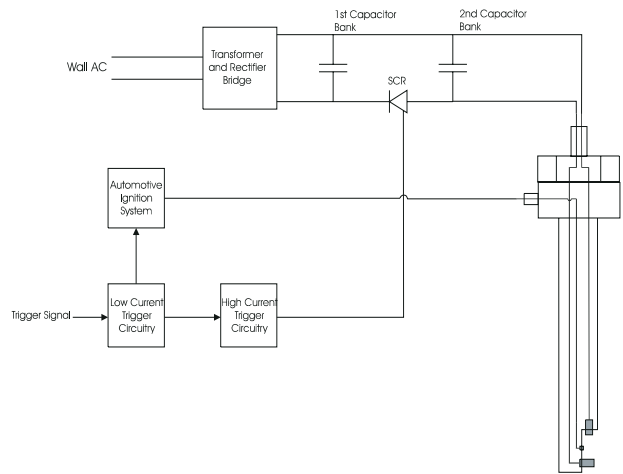


Figure 3. Ignition system schematic figure

Household electricity is transformed and rectified up to 2200 VDC, which is used to charge the first series of capacitor banks. This potential charges the second bank as soon as the silicon-controlled rectifier (SCR) is triggered by the low current circuitry. Once the second discharge capacitor bank is charged, there is a potential of up to 2200 VDC between the pair of large electrodes on the arc plug, shown in figure 4.

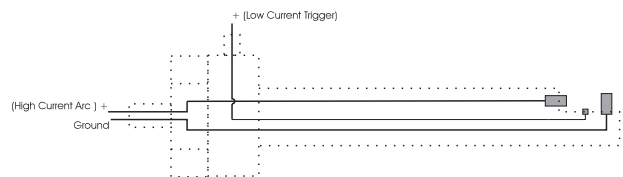


Figure 4. Diagram of high-current arc-plug figure

The gap between the larger electrodes is too great for the second capacitor banks potential to discharge across them. However, when an automotive ignition spark is triggered, a low energy spark is discharged from the smaller electrode to the ground electrode. When this occurs, the path between the high-current anode and

ground electrode becomes ionized to the level where potential breakdown of the discharge capacitor bank is imminent. The triggering sequence takes just over 5ms, which implies an operating frequency up to 200Hz. Single-shot discharge measurements of a 1700 VDC capacitor potential are plotted in figure 5.

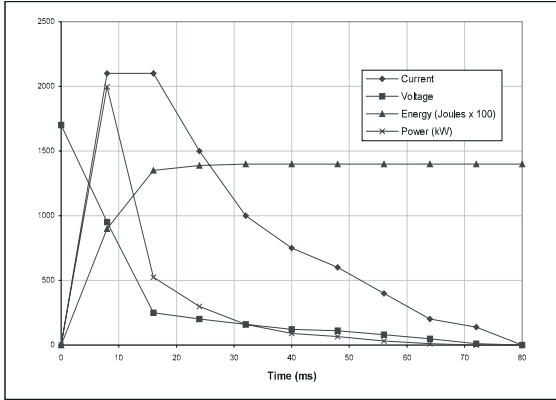


Figure 5. Arc discharge measurements figure

The discharge levels, however, are strongly dependent on the ignition system operation frequency. Figure 6 shows the discharge energy as a function of operation frequency for a 2200 VDC capacitor potential level.

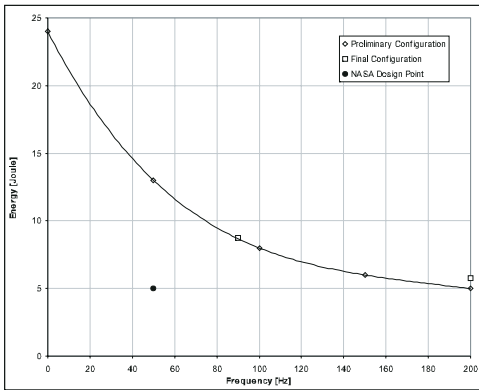


Figure 6. Discharge energy as a function of ignition system operation frequency figure

### Injection System

Tackling the problem of injecting stoichiometric gas species into an intermittent detonation device is a bit more involved than the partial pressure method used when charging up a single shot detonation experiment. Two FlowDyne Corp. critical flow nozzles were used in metering both oxygen and fuel flow rates. Upstream values of pressure and temperature were obtained from transducers. From that information, along with the area ratio of the CD nozzle, a relationship of the following form can be made for both fuel and oxidizer gases:

$$\dot{m} = K(A/A^*, P_1) \frac{P_1}{\sqrt{T_1}} \quad (1)$$

Readings of steady values of  $P_1$  and  $T_1$  are taken upstream of the flow nozzles as illustrated in figure 7.

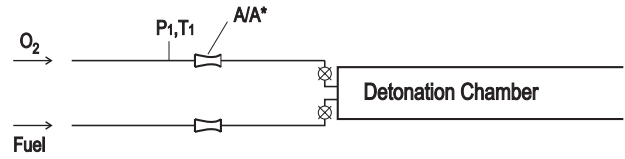


Figure 7. Critical flow nozzle location and terminology schematic figure

Calibration was carried out using cold flows. Choking of the nozzle is crucial for proper measurements. A steady pressure trace should be recorded even as the injection system pulses flow into the chamber. If oscillations occur at the cycle frequency, then the flow nozzles are not choked. After the cold flow calibration is complete, mass flows were measured during hot flow or engine-on conditions. When these mass flows were calculated and confirmed with that of the cold flow tests, then the two pressure transducers and two thermocouples may be removed to free memory for higher resolution or longer duration data sampling.

Caution must be taken when using the measured mass flows because they are metered about 1.5 m upstream of the injection valves. Due to compressibility effects in the remaining tubing downstream of the flow nozzles, the calculated equivalence ratio of the injected species may not be at a stoichiometric value. These mass flows remain estimates. Minor trimming of the regulator pressures from the estimated stoichiometric values can be done until maximum engine performance is obtained.

The fuel and oxygen sources were kept at a reasonable distance from each other as well as the PDR for safety reasons. Flash arrestors were also installed about 15 m upstream of the mass-flow meters to further ensure safety. The reactants were delivered to the detonation chamber via a mechanical rotary valve injection system. This valve was designed and fabricated at UTA for fuel injection, oxygen injection, and purging purposes. Gases were injected from the side opposite the drive gear and then distributed from three ports in a radial fashion from the internal rotating shaft. The three valves are mounted to the engine via a trapezoid shaped manifold as seen in figure 8.

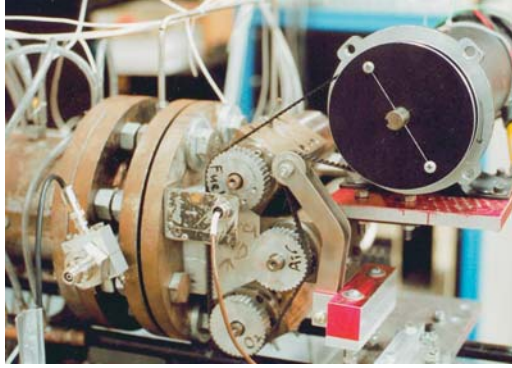


Figure 8. Rotary valve injection assembly

This block directed the propellant and purge flows into the engine from the end wall. The gases are then forced into a swirling motion by an injection disk mounted on the end wall inside the detonation tube to enhance mixing. Due to the present drive gear radius and friction of the rotating system, the 0.5 hp electric motor was only capable of driving the system up to a cycle frequency of 20 Hz.

### Data Acquisition

Data samples were taken through a DSP Technology, Inc. model 9200 12-bit data acquisition unit. This system has separate rack-mountable modules for digitizing, amplification, and storage.

Three main configurations were incorporated. The 100 kHz digitizers, at the maximum 10  $\mu$ s sampling resolution, along with the 512 ksample memory modules were used for initial mass flow calibrations where lower sampling resolution as well as smaller storage space were adequate for simpler data reduction. Another configuration was used for relatively long multi-cycle demonstrations. Again, the 100 kHz digitizers and 512 ksample memory modules were used, but this time the digitizers sampled at 50  $\mu$ s. The final configuration was set up purely for detailed detonation wave analysis. Both of the 4-channel digitizers, set to 1  $\mu$ s were included. To ensure adequate records, the 2.048 Msample memory module had to be used. This limited the sampling window to 250 ms, but due to the enormous file sizes generated, it never was fully reduced. Only the portions of interest in about 10 ms windows were reduced.

## Experiment Results

### Clean Configuration Results at Baseline Regulator Settings

Clean configuration results (figure 1) are from stoichiometric regulator settings at a cycle frequency of 6.9 Hz. Data acquisition was configured for a 1 MHz/channel sampling frequency but because of the large amounts of data produced only a 3 ms window of the wave profile was reduced. Figures 9 and 10 show typify the clean configuration performance of low velocity wave fronts with a reflected shock accelerating from behind.

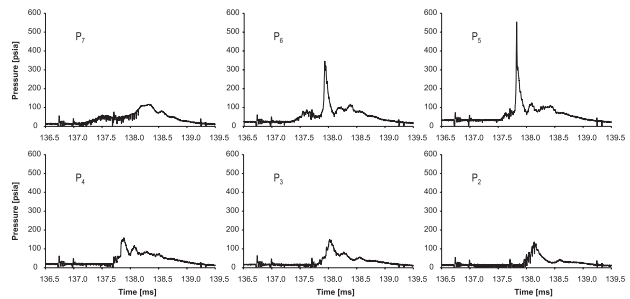


Figure 9. Clean configuration wave profile with 6.9 Hz cycle frequency

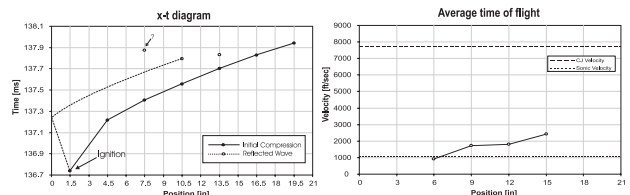


Figure 19. Wave diagram for above test case and average time of flight for all 6.9 Hz test cases

An initial (stage  $P_7$ ) weak compression front is evident in figure 10 shortly after ignition. An overpressure level is generated from the reflection off the end-wall. Recall that the ignition source is mounted 3.8 cm (1.5 inches) downstream from the closed end of the detonation chamber. This reflected shock tends to lose strength as it accelerates towards the leading compression front. By the time the shock front reaches station  $P_4$  34.3 cm (13.5 inches) downstream, it is completely unnoticeable after coalescing with the leading compression front.

The wave diagrams for each wave profile dissection show this wave acceleration and coalescence from another perspective. The leading wave velocity is represented by the solid line discretized between the pressure sensor and ignition locations. The dashed line denotes the assumed path that the reflected wave would take while accelerating towards the initial front. However, one test case shows a point outside of the dashed trend line (figure 10). This location of a shock on an x-t diagram is usually due to the presence of a retonation wave. But no significant detonation front is recognizable in any of the three wave profiles that would form a retonation. An explanation into this event remains unresolved.

Time-of-flight plots are as significant in determining detonation performance as are the pressure wave profiles. No significant velocity levels were measured supporting the evidence of poor performance visible through the wave pressure profiles. Each time-of-flight plot represents the leading compression front only. Every case shows initial average velocity just over the sonic velocity for a 1 atm stoichiometric  $C_3H_8/O_2$  pre-detonation mixture. Even though wave acceleration is clearly evident, velocity levels barely reach 30% of the CJ state by the end of the 53.3 cm (21 in) detonation chamber.

### Shchelkin Spiral Results

The following results pertain to the configuration illustrated in figure 2. Propane and oxygen regulators remain at the calculated stoichiometric baseline setting used for the clean configuration experiments. The only varying parameter is the cycle frequency, which greatly affects the performance of the engine. A range of four cycle frequency settings was chosen from the maximum 20 Hz to a relatively low setting of 4.4 Hz.

#### 20 Hz Cycle Frequency

For the 20 Hz cycle frequency test case the sampling frequency was at 100 kHz/channel due to memory constraints. This was adequate for a cycle-to-cycle repeatability experiment of relative long sampling duration. Cycle-to-cycle repeatability shows significant overpressure levels of around 200 psia on average, albeit lower than the CJ level. The way that the pressure transducer hardware was mounted to the experimental set-up left a small volume between the sensing surface of the transducer and the detonation chamber. This small volume damped out the pressure signal and never allowed the dynamic transducers to register the full shocked level. One way to remedy this problem is to mount the transducer flush to the detonation chamber inside wall. Past experiments using this method exhibited a stronger overpressure profile than that of the water jacket mounted case<sup>6</sup>. However, those tests were done in a single shot mode of operation. For relatively high operation frequencies, it is imperative that water jackets be used for protecting the pressure transducers.

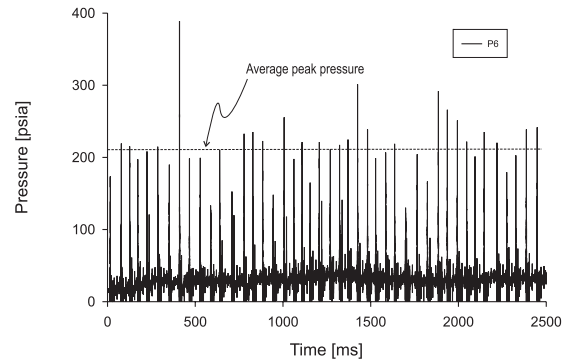


Figure 11. Chamber pressure history at 20 Hz figure

A more in-depth performance evaluation can be done by zooming into an individual wave profile. In the region of the Shchelkin spiral's influence, the wave shows significant transition towards a detonation front in overpressure levels as well as average velocities. However, the wave tends to weaken considerably as it propagates towards the open end. Although each of the forty to fifty individual wave profiles shows poor performance (figure 12), the consistent intermittent overpressure history (figure 11) encourages support for the use of the Shchelkin spiral in higher frequency modes of operation.

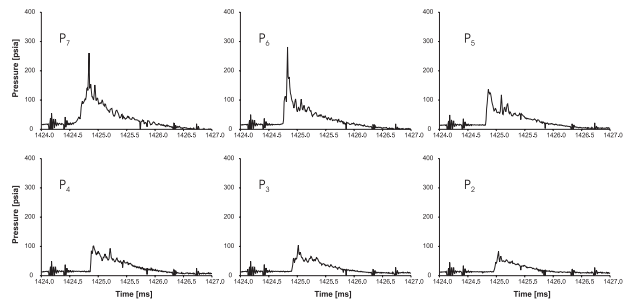


Figure 12. Typical wave profile from 20 Hz test case

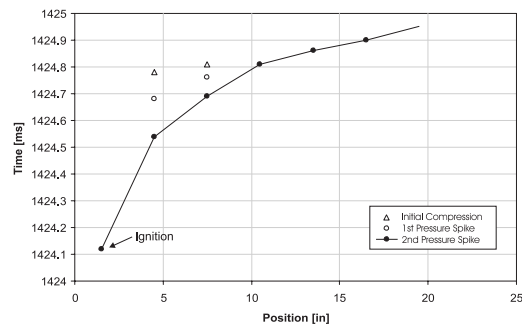


Figure 13. Wave diagram for 20 Hz test profile from figure 12

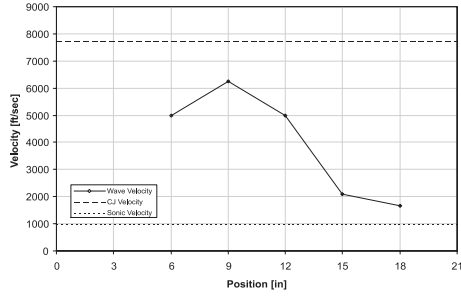


Figure 14. Average velocity plot for 20 Hz test in figure 12

### 14.4Hz Cycle Frequency

The next test example is from a 14.4 Hz cycle frequency test case. Sample frequency was also set at 100 kHz for the purpose of adequate memory for long sampling durations. Cycle to cycle repeatability is illustrated in figure 15.

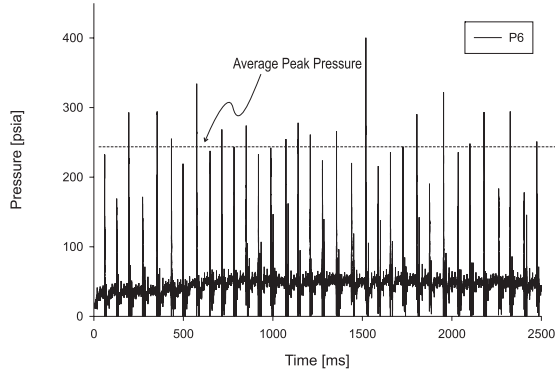


Figure 15. Chamber pressure history from 14 Hz test case figure

Again, significant cycle-to-cycle overpressure levels are demonstrated. Average peak pressure is slightly higher than that of the 20 Hz case. Upon zooming in (see figure 16) the same early transition trend can be seen in the region of the spiral. However, after the end of the spiral,  $P_3$  the profile shows a higher pressure peak than in the 20 Hz case, as evident in Figure 18.

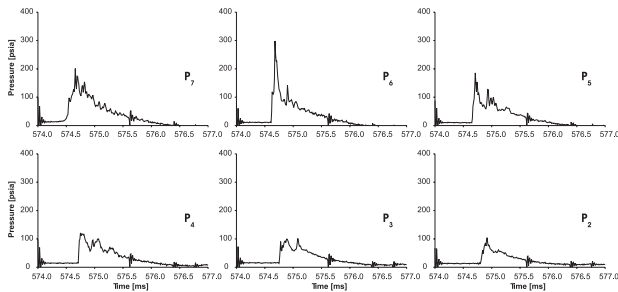


Figure 16. Typical wave profile from 14.4 Hz test Case figure

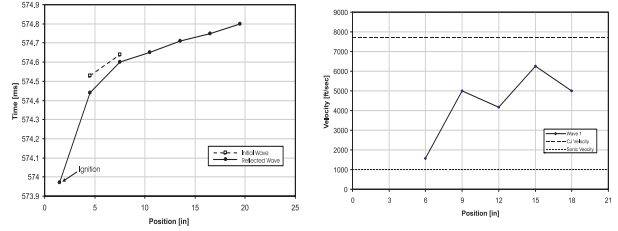


Figure 17. Wave diagram and average velocity plot for 14.4 Hz test in figure 16

### 6.9 Hz Cycle Frequency

The DAQ hardware configuration was changed to allow a 1 MHz sampling resolution with a purpose to significantly resolve the wave profile. Sample times were around 250 ms and created massive data files. Only 3 ms windows around the wave profiles of interest were reduced to simplify the post-processing of the data. No macroscopic cycle-to-cycle demonstration was available for any case with the 1 MHz sampling resolution because of the modification. Figure 18 is the profile from the 6.9 Hz test case. Two peaks are clearly visible, a leading overpressure followed closely by a reflected front. Both are mapped in the Wave diagram of figure 20.

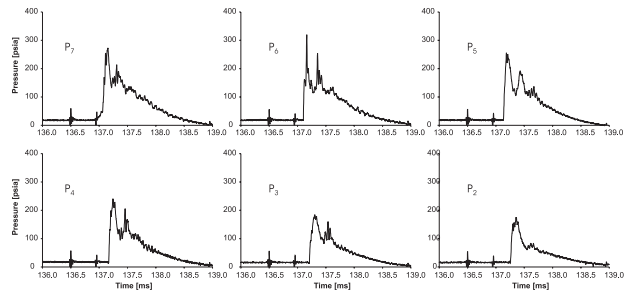


Figure 18. Typical wave profile from 6.9 Hz test Case figure

A significant trend is now beginning to develop. Not only is there rapid transition into a detonation profile in the Shchelkin spiral region, but there is also considerable sustentation after the wave passes the obstacle. Peak average velocities even reach the CJ level in the region of the spiral (figure 20), a characteristic obviously absent in higher frequency cases.

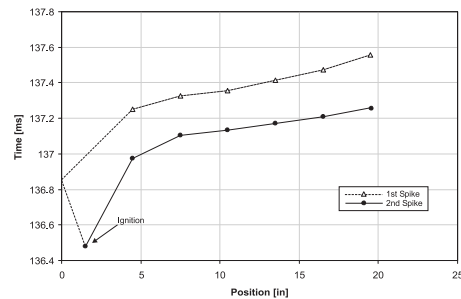


Figure 19. Wave diagram for 6.9 Hz test in figure 18



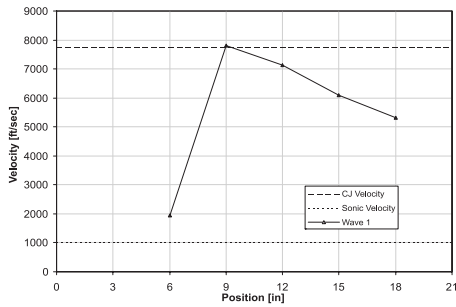


Figure 20. Average velocity plot for 6.9 Hz test in figure 18

#### 4.4Hz Cycle Frequency

Again, with the DAQ sample resolution at 1 MHz, only the resolved individual wave profiles are available for the 4.4 Hz cycle frequency tests. This is the lowest cycle frequency test case recorded and shows the best performance of all the frequency settings. Not only did the Shchelkin spiral demonstrate a detonation wave being generated in a relatively short distance, 11.4 to 19.1 cm (4.5 and 7.5 in), but it also shows that the wave can sustain itself to the end of the 53.3 cm (21 in) chamber with only minor velocity level decline.

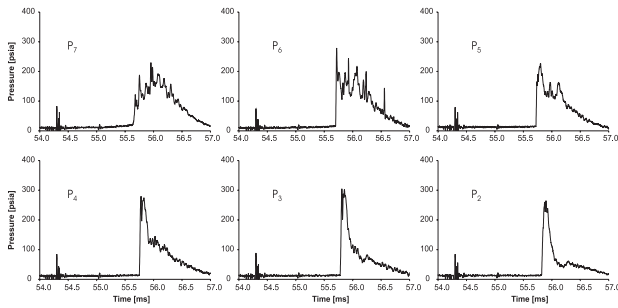


Figure 21. Typical wave profile from 4.4 Hz test Case figure

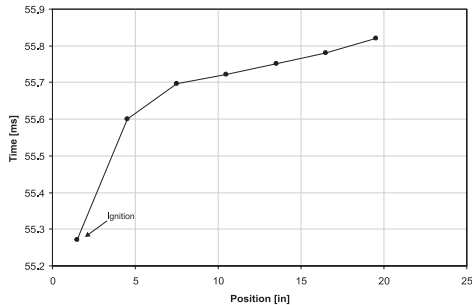


Figure 22. Wave diagram for 4.4 Hz test in figure 21

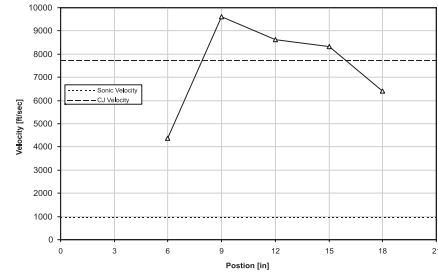


Figure 23. Average velocity plot for 4.4 Hz test in figure 21

#### Discussions

Significant lack of performance was observed with the clean configuration at a modest cycle frequency of 6.9 Hz. Not a single detonation was achieved and velocity levels barely peaked at 30% of the CJ level. Several reasons may be the cause of this problem. One possibility is that the length of tubing between the mass flow meters and the injection valving created non-stoichiometric levels upon injection into the detonation chamber. In addition, the problem of adequate mixing was not tackled. Figure 25 shows that at 6.9 Hz, only about a 40 ms window (the time after the injection valve closed to the time of ignition) would be available for mixing. The swirling disc used to enhance mixing may not be creating the desired level of turbulence to completely mix the  $C_3H_8/O_2$  gases in such a short period.

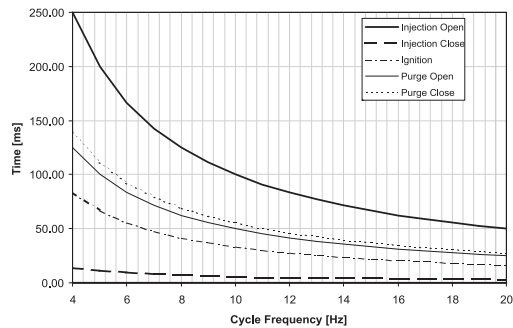


Figure 24. Injection and ignition timing as a function of cycle frequency

The clean configuration profile shows poor performance early in comparison to the wave profile of the Shchelkin spiral case with identical run conditions at 6.9 Hz. To the untrained eye, it is very difficult to see any improvement in wave profile beyond that. But, upon looking closer at the profiles from  $P_6$ ,  $P_5$ , and  $P_4$  for the Shchelkin spiral case (see figure 18), there is a considerably distinct pressure spike which is characteristic of shocked flow. At every location for the clean configuration case, an obvious pre-compression is evident before the large overpressure level.

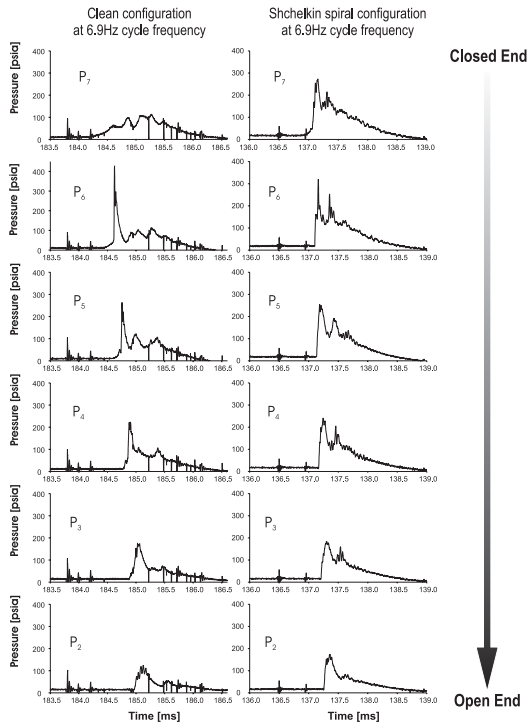


Figure 25. Clean and Shchelkin spiral configuration pressure profile comparison results at 6.9 Hz cycle frequency figure

Improved performance in the Shchelkin spiral configuration is even more obvious in the time-of-flight plot of figure 26. The wave consistently reaches a CJ level in a short distance near the end of the Shchelkin spiral. This velocity lasts only for a short distance before the lack of fill in the chamber begins to take effect.

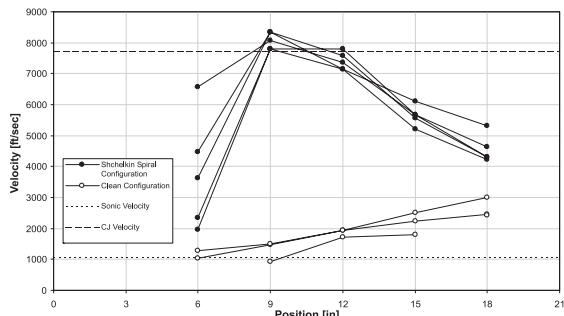


Figure 26. Clean and Shchelkin spiral configuration velocity comparison at 6.9Hz cycle frequency figure

Fill time due to cycle frequency did posed an egregious problem in the ability to sustain a detonation through the length of the chamber. Figure 27 combines profile plots from the 20, 14.4, 6.9, and 4.4 Hz cycle frequency test cases with the Shchelkin spiral installed. The characteristic shocked flow profile becomes much more visible toward the open end of the tube as the cycle

frequency is reduced, with a corresponding increase in injection and mixing times.

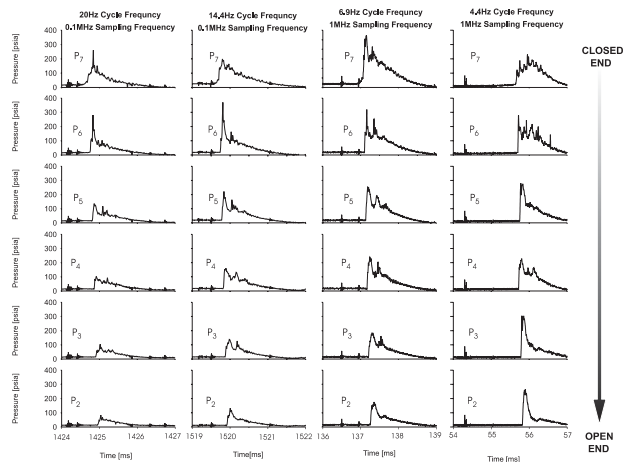


Figure 27. Single pulse propagation comparison at varied frequencies figure

This varied frequency effect is just as evident in the time-of-flight plot of figure 28. Cases of five different cycle frequencies are superimposed on the same plot illustrating the difficulty of achieving high velocities at high frequencies. Significant average velocities above or near the CJ level occur in the lower frequency cases. Higher cycle frequency velocities fall short of that plateau and tend to ebb off much more sharply.

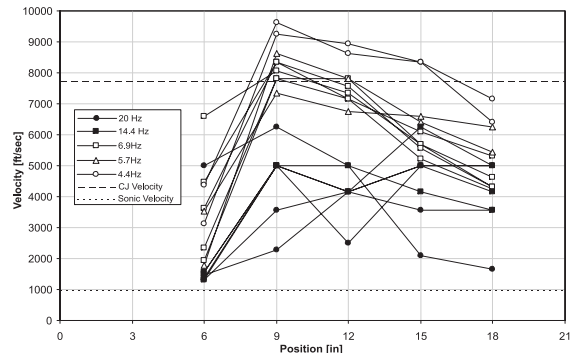


Figure 28. Average velocity plot for Shchelkin spiral installed configuration

## Conclusions

Detonations are readily obtained in a very short distance, 11.3 to 17.5 cm (8 to 10 in), for modest cycle frequencies of 4.4 and 6.9 Hz with the Shchelkin spiral installed. This is apparent through the time-of-flight plots that show high velocity levels near or above the CJ level for the standard atmosphere pre-detonation condition. Although the pressure profile plots show pressure spikes



lower than that of CJ level (due to the method of installing the pressure transducers), they do show sharp shocked profiles with hardly a sign of pre-compression except in early stages of transition.

At higher frequencies, 14.4 and 20 Hz, only strong intermittent overpressures are observed. Each pressure profile yielded weak pre-compressions followed closely with a relatively strong overpressure peak that quickly deteriorated after passing the Shchelkin spiral. Average velocity plots are consistent with this diminishing of the wave front as velocity falls off towards the end of the chamber, never reaching the CJ level. This is possibly due to improper filling of the detonation chamber from cycle to cycle which is a major argument for the improved performance at lower frequencies.

An explanation into the drastic increase in the Shchelkin spiral case may be poor mixing. The clean configuration showed velocity levels at around 30% of the CJ level. The Shchelkin spiral possibly added beneficial mixing effects as well as reducing DDT lengths.

The configuration of the PDR for this report showed poor performance at high frequencies. However, cycle to cycle repeatability was shown in the Shchelkin spiral configuration with better results than that of the clean configuration. A method of injection must be redesigned to allow more mass of gases for each cycle regardless of operating frequency.

The largest obstacle of this experiment was the injection system. At high frequencies, only small slugs of gases could be injected each cycle. This was due to the coupling of the rotary valves and drive motor which dictated cycle frequency. Two main recommendations could remedy this problem. The volume of the chamber may be unnecessarily large. Money constraints limited purchasing and upgrade options so the old 2295 cm<sup>3</sup> (140 in<sup>3</sup>) chamber was used. This chamber has an inside diameter of 7.6 cm (3 in) which is excessively larger than the cell size of a propane-oxygen detonation which is under 0.5 cm at a standard atmosphere pre-detonation condition. Decreasing the chamber volume to a tube of 2.54 cm (1 in) diameter (still significantly larger than the detonation cell size) with the same length of 21 in would reduce cycle to cycle propellant mass requirements by a factor of 9.

Another fix would be to eradicate the rotary valve system and develop a solenoid valve one instead. Digitally controlling the injection duration would alleviate the coupling of injection and cycle frequency. Consideration has been given to this improvement, but finding solenoid valves that can deliver enough mass at the high frequencies desired has been challenging<sup>7</sup>.

## References

1. Zeldovich, I. B., Kompaneets, A. S., "Theory of Detonation," Academic Press, New York, 1960.
2. Kailasanath K (2000) AIAA J 38(9):1698-1708
3. Kiyanda CB, Tanguay V, Higgins AJ, Lee JHS (2002) J Propulsion and Power 18(5):1124-1125
4. Litchford RJ (2001) AIAA Paper 2001-3814
5. S.-Y. Lee, C. Conrad, et. al, "Deflagration to Detonation Transition Study Using Simultaneous Schlieren and OH PLIF Images," AIAA Paper 2000-3217, 36th AIAA/ASME/SAE/ASEE Joint Propulsion Conference, AIAA, Huntsville, Alabama, 2000.
6. Stanley, S., Stuessy, W., S. and Wilson, D. R., "Experimental Investigation of Pulse Detonation Wave Phenomenon," AIAA Paper 95-2197, 1995.
7. F.K. Lu, D.S. Jensen, "Potential of a Fast-Acting Micro-Solenoid Valve for Pulsed Detonation Fuel Injection," AIAA Paper 2003-0888, 41<sup>st</sup> AIAA Aerospace Sciences Meeting, AIAA, Reno, Nevada, 2003.